

Article

# Chitosan Based Regenerated Cellulose Fibers Functionalized with Plasma and Ultrasound

Urška Vrabič Brodnjak <sup>1</sup>, Adolf Jesih <sup>2</sup>  and Diana Gregor-Sveteč <sup>1,\*</sup>

<sup>1</sup> Faculty of Natural Sciences and Engineering, Department of Textiles, Graphic Arts and Design, University of Ljubljana, Snežniška 5, SI-1000 Ljubljana, Slovenia; urska.vrabc@ntf.uni-lj.si

<sup>2</sup> Jožef Stefan Institute, Jamova cesta 39, SI-1000 Ljubljana, Slovenia; Adolf.Jesih@ijs.si

\* Correspondence: diana.gregor@ntf.uni-lj.si; Tel.: +386-1-200-32-72

Received: 7 February 2018; Accepted: 4 April 2018; Published: 5 April 2018



**Abstract:** The great potential of regenerated cellulose fibers, which offer excellent possibilities as a matrix for the design of bioactive materials, was the lead for our research. We focused on the surface modification of fibers to improve the sorption properties of regenerated cellulose and biocomposite regenerated cellulose/chitosan fibers, which are on the market. The purpose of our investigation was also the modification of regenerated cellulose fibers with the functionalization by chitosan as a means of obtaining similar properties to biocomposite regenerated cellulose/chitosan fibers on the market. Argon gas plasma was used for fiber surface activation and chitosan adsorption. Ultrasound was also used as a treatment procedure for the surface activation of regenerated cellulose fibers and treatment with chitosan. Analyses have shown that ultrasonic energy or plasma change the accessibility of free functional groups, structure and reactivity, especially in regenerated cellulose fibers. Changes that occurred in the morphology and in the structure of fibers were also reflected in their physical and chemical properties. Consequently, moisture content, sorption properties and water retention improved.

**Keywords:** chitosan; regenerated cellulose fibers; surface modification; plasma; ultrasonic treatment

## 1. Introduction

Over the past years, chitosan, a natural product with a wide range of advantageous properties, has gone through a great development, becoming successfully integrated into different fields of material science. The use of chitosan in textiles was investigated by much research, where antimicrobial, tensile and water absorption properties were the most important properties to study [1–6]. Chitosan is a commonly used biopolymer, with unique chemical and physical properties. It is produced by deacetylation of chitin, which is a biodegradable, nontoxic polysaccharide that is water-soluble in acid, amongst others [2–5]. It has many applications in pharmacy, biotechnology and cosmetic industry [2,3]. Cellulose and chitosan have similar molecular structures, with the same  $\beta$ -glycoside linkages. The main difference is the presence of primary amino groups at the C-2 positions in chitosan, where the cellulose has hydroxyl groups. The presence of active groups in the chitosan molecular structure allows for easy chemical modification [3–5]. These groups are responsible for its solubility in a diluted aqueous acid solution as a polycationic polymer [4–7]. Many studies were done regarding different applications of chitosan, especially on chitosan blends with cellulose [3–6].

Regenerated cellulose fibers are cleaner and more hygroscopic than cotton, and they are highly applicable to hygiene and medical products [7,8]. The major features of regenerated cellulose fibers include a variable morphology and variable physical properties, softness, good processing characteristics, adequate liquid transport properties and good mechanical properties [4,6,9–14]. In recent decades, many applications of regenerated cellulose fibers have been developed, not only as

clothing but also as medical and sanitary products, for which a high uptake of aqueous fluids is part of the essential performance requirements [10–12,15]. A cellulose polymer consists of three hydroxyl groups per anhydrous glucose unit, and these groups attract water; thus cellulose is characterized by a relatively high moisture absorption [7,13]. In order to enhance absorption properties further, many studies have been conducted and a variety of techniques have been utilized [4,7,13,14]. These methods mainly focused on chemical or mechanical treatments [8–12].

Some wet textile pre-treatment and finishing processes like enzymatic treatments are also widely used to improve the softness and physical properties of textiles and fibers. Such treatments are less ecologically friendly than plasma or ultrasound, where no additional chemicals are needed. Many techniques are available for applying chitosan to cellulose fibers, such as treatments of cellulose fibers with cross linking agents, where cotton fibers are soaked in chitosan solutions [7,8,12–14]. In recent years, many studies have been made on cellulose fibers that are functionalized with chitosan [4–10,12–21]. Chitosan treatments offer many advantages for regenerated cellulose fibers, such as biodegradability, non-toxicity, improved absorption ability, etc. [12–17]. In our research, plasma and ultrasound were used as treatment techniques. Plasma treatment is a fast, solvent-free technique, where the procedure is simple and well controlled. It causes changes at a limited depth, modifying atomic layers of a material's surface. With this technique, the bulk characteristics stay unaffected, even for very sensitive and fragile materials [22–25]. With ultrasound treatment, chemical and physical processes could be conducted, mainly due to the ultrasonic cavitation effect in a liquid medium [26–28]. The breakage of chemical bonds, and the improvement of their accessibility and reactivity are one of the biggest impacts on the material's molecular structure [28,29]. It is an environmentally friendly process and efficient in many surface treatments [27–30].

Our research focused on ultrasound and plasma treatments of regular regenerated cellulose fibers and biocomposite regenerated cellulose/chitosan fibers, with the goal of enhancing their sorption properties. Another main aspect of our research was the functionalization of regenerated cellulose fibers by chitosan in order to obtain properties similar to biocomposite regenerated cellulose/chitosan fibers, which are on the market.

## 2. Materials and Methods

### 2.1. Materials

In this study, two types of regenerated cellulose fibers were used: pure cellulose and biocomposite cellulose fibers. Both regenerated cellulose fibers were made using a viscose manufacturing process. Lenzing Viscose<sup>®</sup>, from Lenzing AG, Lenzing, Austria, also known as viscose rayon fiber, had a declared value of linear density of 3.0 dtex and a length of 29 mm. Biocomposite regenerated cellulose/chitosan fibers Crabyon<sup>®</sup> were obtained from Omikenshi Co. Ltd., Osaka, Japan. The declared value of the linear density and the length of these fibers was 2.8 dtex and 28 mm.

A chitosan solution, which was applied onto the regenerated cellulose fibers, was prepared by dissolving 3 g of chitosan in 2% aqueous acetic acid at 60 °C. Chitosan (molecular weight 50 kDa, acetylation degree 85%) was purchased from Sigma Aldrich, Austria. Acetic acid (99.8% assay) was purchased from Sigma Aldrich, Vienna, Austria.

### 2.2. Ultrasound Treatment

The regenerated cellulose fibers and biocomposite regenerated cellulose/chitosan fibers, were first washed in a bath containing 1 g/L of non-ionic surfactant with a liquor ratio of 20:1 for 60 min and dried in a laboratory oven for 4 h at 104 °C. After the drying, samples were separately treated in an ultrasound bath for 120 min, under a constant frequency of 40 kHz. The power density, for a liquid volume of 200 mL, was 0.064 W/mL. After the treatment procedure, they were washed via the same procedure as at the beginning, then dried in the air for 12 h before being dried in a laboratory oven at 50 °C for 1 h.

The regenerated cellulose fibers were also immersed in the chitosan solution and treated in an ultrasound bath following the same procedure.

### 2.3. Plasma Treatment

Before the plasma treatment, the regenerated cellulose fibers and biocomposite regenerated cellulose/chitosan fibers were first washed in a bath containing 1 g/L of non-ionic surfactant with a liquor ratio of 20:1 for 60 min and dried in a laboratory oven for 4 h at 104 °C. After drying, samples were immersed into a prepared chitosan solution, as described. Fibers were immersed for 120 min at 60 °C. After that, washing with hot (60 °C), warm (30 °C) and cold water continued. After that, the samples were washed via the same procedure as at the beginning. Fibers were then dried in the oven at 50 °C for 1 h.

Experiments were carried out in a bell jar type Pyrex reactor with 150 mm o.d. and that was 200 mm in length. The source of radio-frequency power was an IEVT VGK 200/1 high frequency generator operating at 27 MHz and at 300 W maximum power. The power dissipated in the plasma reactor was measured by a Zetagi HP 201 SWR through-line wattmeter (Thunderpole, Northampton, UK). The plasma was inductively coupled through a coil, and the pressure in the reactor was measured via a pressure meter. Argon gas was supplied to the reactor from a gas cylinder, and the flow was controlled by mass controllers. First the system was pumped down to  $10^{-3}$  Pa, and after fibers were put in the reactor the system was evacuated to a pressure level of 100 Pa. The flow rate of argon was adjusted to  $10 \text{ cm}^3 \text{ min}^{-1}$ , and the system was allowed to flush with argon. After flushing for 2.5 min, pressure stabilized and the plasma was initiated. After a 5-min treatment of fibers at the argon flow rate of  $10 \text{ cm}^3 \text{ min}^{-1}$ , a flow rate of  $50 \text{ cm}^3 \text{ min}^{-1}$  was applied for another 5 min respectively.

All samples and treatments in this research, are presented in Table 1.

**Table 1.** Notation of untreated and treated regenerated cellulose and biocomposite regenerated cellulose/chitosan fibers.

Sample	Fibers	Type of Treatment
V	Regenerated cellulose fibers	Untreated
V-ultras.	Regenerated cellulose fibers	Ultrasound
V-plasma	Regenerated cellulose fibers	Plasma
C	Biocomposite regenerated cellulose/chitosan	Untreated
C-ultras.	Biocomposite regenerated cellulose/chitosan	Ultrasound
C-plasma	Biocomposite regenerated cellulose/chitosan	Plasma
V/CH-ultras.	Regenerated cellulose fibers	Chitosan+ultrasound
V/CH-plasma	Regenerated cellulose fibers	Chitosan+plasma

### 2.4. Molecular and Supramolecular Properties

The degree of polymerization, crystallinity and molecular orientation of the untreated and treated fibers was investigated.

The degree of polymerization (DP) was determined using the viscosimetric method, according to the Schulz-Blaschke equation [13]. The DP of the samples dissolved in Cuoxam was determined using an Oswald shear dilution viscometer. In our research, four parallel measurements were done for each type of tested fiber.

To determine the crystallinity of the fibers from iodine sorption, the Schwertassek method was used [4,13]. The fibers were first treated with  $\text{KJ}_3$  solution, after which the concentration of non-absorbed iodine was determined by titration. Four parallel measurements were done for each type of tested fiber. The iodine sorption value (IS) is the amount of iodine adsorbed by one gram of cellulose substrate. It was calculated via the following equation:

$$IS = (a - b \cdot 1.33) \cdot F \cdot 2.5384/m \quad (1)$$

where  $a$  is the volume [mL] of  $\text{Na}_2\text{S}_2\text{O}_3$  solution ( $c = 0.01$  mol/L) for a liquor of blank KI solution,  $b$  is the volume [mL] of  $\text{Na}_2\text{S}_2\text{O}_3$  solution ( $c = 0.01$  mol/L) for a liquor of sample solution,  $c$  is a constant (for cellulose: 1.33),  $F$  is a liquor factor of  $\text{Na}_2\text{S}_2\text{O}_3$  solution, determined by  $\text{KMnO}_4$  (0.02 mol/L), and  $m$  is the weight of absolutely dry fiber sample [g]. From the given values of iodine sorption for amorphous cellulose ( $IS = 412$  mg/g), the proportion of the amorphous ( $x_a$ ) and crystalline ( $x_c$ ) phases was calculated [13].

The average molecular orientation was determined from the birefringence measurement. The birefringence of the fibers was determined using a Meopta polarizing light microscope () and an Eringhaus compensator. In our research, 50 measurements were done for each type of tested fiber.

Fourier transform infrared spectroscopy (PerkinElmer, Waltham, MA, USA) was used to determine the chemical structure of the treated and untreated fibres. The spectra were recorded over the range  $4000\text{--}800$   $\text{cm}^{-1}$ , with a resolution of  $4$   $\text{cm}^{-1}$ .

### 2.5. Moisture and Water Sorption Properties

The reactivity and sorption ability of the fibers were analyzed using various standard methods. The moisture content of the fibers was determined after 4 h of drying at  $105$   $^\circ\text{C}$ , according to the standard SIST EN 20139:1999 [4].

The capability of water retention was determined according to the standard ASTM D 2402-90 [4]. The standard method determines a ratio between the mass of water retained in the fibers after soaking (for 2 h) and centrifuging for 20 min, and the mass of dried fibers (temperature  $105$   $^\circ\text{C}$ , 4 h).

The liquid absorptive capacity and liquid absorbency time (ASTM D 1117-80 [4]) were determined as the time the basket filled with 5 g of fibers required to sink below the surface of the distilled water. After the sample was removed from the water and dried for 30 s, the difference in weight gave the absorptive capacity.

### 2.6. Tensile Properties

The tensile properties of the fibers were determined in the standard atmosphere, at a temperature of  $20$   $^\circ\text{C}$  and with 65% relative air humidity, using the tensile testing machine Instron 6022 (Illinois Tool Works Inc., Newburyport, MA, USA). The cross-head speed was  $0.15$  mm/s, the pre-loading was  $0.5$  cN/dtex and the gauge length was  $2.5$  mm. During the fiber stretching, several load and elongation data were recorded per second, until the fiber broke. We obtained an average curve from the measured load and elongation data. The average curve was then converted into a stress-strain curve. The tensile data presented in this article were obtained from the average of 50 fibers.

### 2.7. Thermal Stability

The temperature of fiber degradation was determined via sample inspection with the Mettler FP84HT Hot stage thermal measuring cell.

### 2.8. Surface Morphology

The efficiency of the ultrasound or plasma treatment of fibers, as well as of the functionalization by chitosan was examined via scanning electron microscopy (SEM). The SEM micrographs were taken on the JSM-6060LV instrument, which was operated at  $10$  kV.

## 3. Results and Discussion

### 3.1. Structural Characteristics

In Table 2, the molecular and supramolecular properties of the untreated and treated fibers are presented. As expected, the untreated regenerated cellulose fibers have a higher degree of polymerization, crystallinity and orientation of macromolecules, compared to the biocomposite regenerated cellulose/chitosan fibers. Ultrasound or plasma treatments caused the lowering of

the molecular orientation, and the supramolecular structure became less ordered, which was seen in all the ultrasound and plasma treated fibers. Both treatment methods give similar results: a decrease of crystallinity, polymerization and molecular orientation in the fibers. Shorter macromolecules on average (DP), less oriented macromolecules ( $f_{or}$ ) and a less ordered crystalline structure indicate that the amount of ordered crystalline areas ( $x_c$ ) in the fibers should also be smaller. This was seen in particular in the regenerated cellulose fibers treated with chitosan, plasma and ultrasound, where the largest decrease of all structural characteristics was detected. It is assumed that the cleavage of cellulose molecules starts in the amorphous regions, releasing cellulose fragments, lowering the degree of polymerization and the orientation of macromolecules, before this is followed with the cleavage of the accessible cellulose molecules on the surface of crystalline regions [13]. The results suggest that both treatments, ultrasound and plasma, stimulated the interactions between chitosan and regenerated cellulose fibers. Hua et al. found that argon plasma treatments initiate reactions mainly associated with the cleavage of C<sub>1</sub>–C<sub>2</sub> linkages in cellulose, leading to the formation of C=O groups [31]. The adsorption of chitosan onto cellulose can be driven by non-electrostatic attractions, such as hydrogen bonds between amino groups and functional groups of cellulose such as carbonyl and carboxyl groups.

**Table 2.** Degree of polymerization (DP), crystallinity ( $X_c$ ), molecular orientation ( $f_{or}$ ) of fibers; s-presents the standard deviation.

Sample	DP	s	$X_c$ (%)	s	$f_{or}$	s
V	510.58	0.25	75.50	0.27	0.4457	0.0388
V-ultras.	485.63	0.69	75.17	0.56	0.3584	0.0254
V-plasma	408.65	1.00	74.41	0.71	0.3321	0.0287
C	458.40	0.88	74.07	0.48	0.4603	0.1446
C-ultras.	441.27	0.75	69.75	0.34	0.3359	0.1147
C-plasma	410.36	0.87	70.82	0.93	0.3778	0.0416
V/CH-ultras.	439.76	0.36	62.59	0.28	0.3639	0.0585
V/CH-plasma	437.88	0.47	67.58	0.88	0.3427	0.0769

A comparative analysis of the treated and untreated regenerated cellulose fibers has shown some differences in their spectra (Figure 1). Due to the absorption band at 1654 cm<sup>-1</sup> assigned to C=O stretching of the secondary amide of chitosan, the absorption band around 1618 cm<sup>-1</sup> assigned to the N–H banding in the primary amine and the absorption band at 1556 cm<sup>-1</sup> indicating the vibrational mode of amide II, the presence of chitosan was detected in the treated fibers [4]. The emerged new absorption bands provided evidence that chitosan was chemically attached to the surface of the regenerated cellulose fibers. It is also evident from the results we obtained that plasma and ultrasound affect the structure of fibers functionalized by chitosan in a similar way, with changes in the molecular-scale behavior of the regenerated cellulose fibers. Ultrasound treatment has a higher impact on lowering the degree of crystallinity, whereas plasma treatment lowers the average molecular orientation more. Figure 1 shows a shift in the peak for the samples treated with ultrasound V-ultras. and C-ultras., from 2890 cm<sup>-1</sup> to 2891 and 2892 cm<sup>-1</sup>, representing ring C–H vibrations, which were shifted to lower absorbencies after the ultrasound treatment. For the plasma treated samples, the peak at 1155 cm<sup>-1</sup> shifted to 1158 cm<sup>-1</sup>, indicating a shortening of the C–O–C glycosidic bond [32]. The peak shift from 3314 cm<sup>-1</sup>, for the untreated samples, to 3326–3330 cm<sup>-1</sup>, for the plasma treated samples with lower absorbencies, represented a shortening and lengthening of the O<sub>3</sub>H···O<sub>5</sub> and O<sub>2</sub>H···O<sub>6</sub> intermolecular hydrogen bonds, respectively [32]. For both ultrasound and plasma treatments, a shift in peaks and lower absorbencies were detected.



retention; chitosan is a big molecule that cannot easily enter into fibers and that is adsorbed mostly on the fiber surface. Morphological changes were detected, but chitosan caused some kind of closing of the porous structure and lowered the specific surface area. This effect could explain the higher liquid absorbency and lower water retention capability.

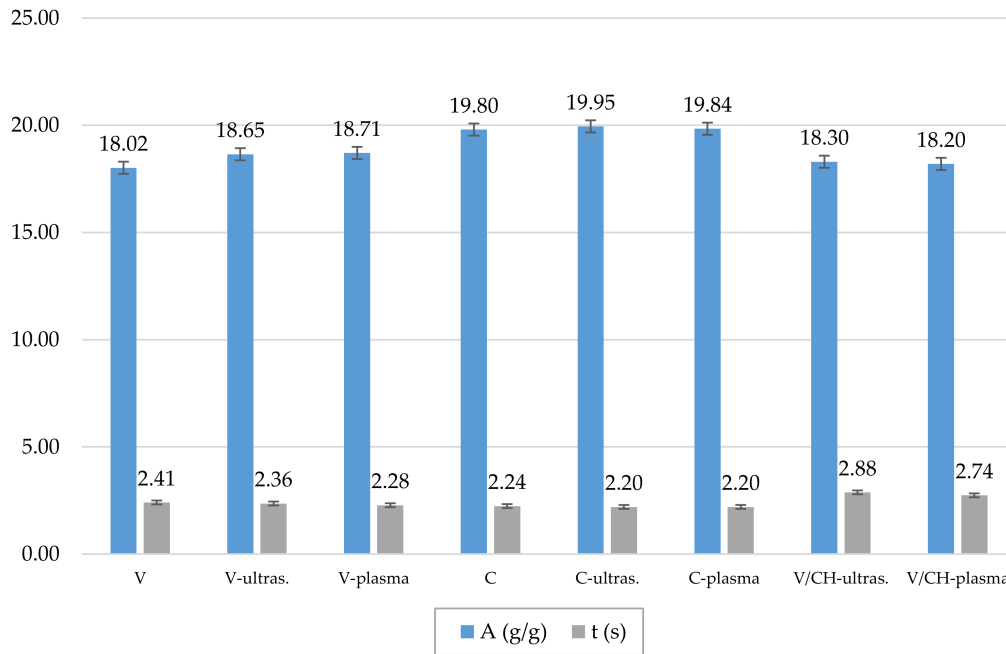


**Figure 2.** Absorptive capacity (*A*) and liquid absorbency time (*t*), for all tested fibers, with the standard deviation.

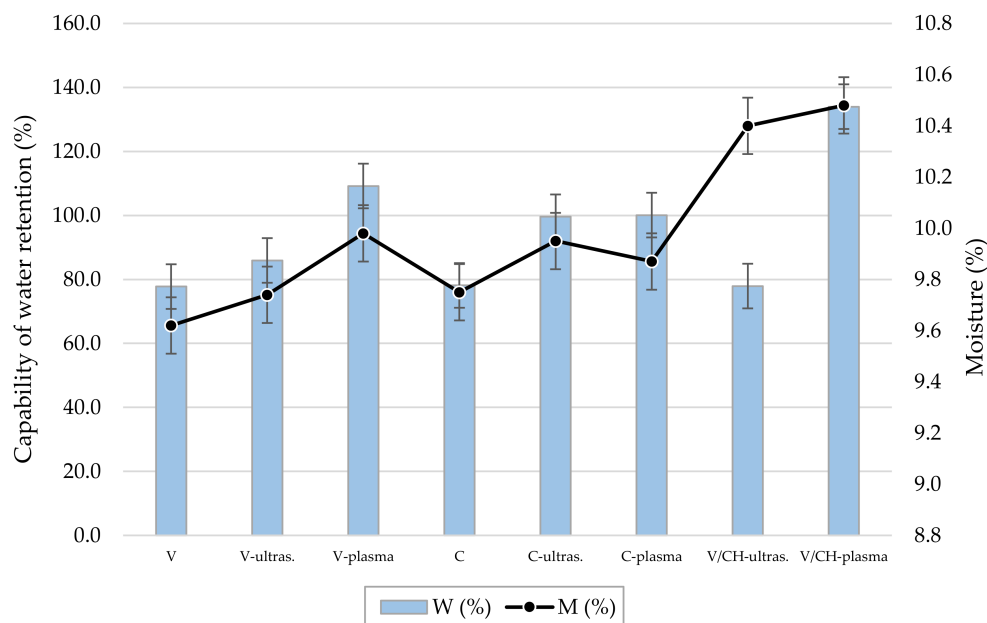


**Figure 3.** Moisture sorption (*M*) and capability of water retention (*W*), for all tested fibers, with the standard deviation.

### 3.3. Tensile Properties

Tensile properties depend on the degree of crystallinity, the degree of polymerization and the orientation of macromolecules in crystalline and amorphous regions of fibers. In Table 3, the tensile properties of the untreated and treated fibers are shown. In general, the influence of different treatments on tensile properties of fibers is quite small, with changes in tenacity of up to 10%. As the depolymerisation of macromolecules first occurs in amorphous regions, this improves hygroscopic properties without a loss of strength, due to strength being mainly determined within the crystalline regions. Shorter macromolecules, a less ordered structure and the intermolecular interactions between chitosan and cellulose can all weaken the hydrogen bonds and interactions between cellulose molecules, resulting in macromolecules stretching more easily, which leads to an increase in tensile elongation. Treatments with ultrasound or with plasma and chitosan have a greater influence on the properties determined when lower loads are applied to fibers, than they do on tensile properties determined at break. With the treatment, the yield stress and elastic modulus are lowered, meaning that resistance to initial stretching is lowered and the onset of the first permanent deformation starts at lower loads. Because of the ultrasound, plasma and chitosan treatment, the fibers are more sensitive to a tensile load and are more easily deformed than are untreated fibers. The most evident change is in elastic modulus, where a decrease of up to 50% was obtained. For all the treated fibers, the strain at break increased, especially for the regenerated cellulose fibers with applied chitosan and plasma treatments (40%). Clearly, the addition of chitosan in the treatment of the regular cellulose fibers had no influence on the fibers' strength, though it influenced the deformability and lowered the resistance to deformation.

**Table 3.** Tensile properties: stress at break ( $\sigma$ ), strain at break ( $\epsilon$ ), yield stress ( $\sigma_y$ ), elastic modulus ( $E_0$ ) of fibers; s-presents the standard deviation.

Sample	$\sigma$ (cN/dtex)	s	E (%)	s	$\sigma_y$ (cN/dtex)	s	$E_0$ (GPa)	s
V	2.51	0.60	33.20	2.00	0.80	0.02	4.59	0.21
V-ultras.	2.48	0.19	35.82	1.07	0.72	0.04	4.25	0.45
V-plasma	2.28	0.81	37.64	0.87	0.73	0.10	3.89	0.36
C	2.15	0.77	36.71	1.05	1.30	0.04	6.52	0.32
C-ultras.	2.85	0.65	39.23	0.97	1.24	0.08	3.55	0.74
C-plasma	2.86	0.54	41.76	0.89	1.38	0.09	3.84	0.65
V/CH-ultras.	2.61	0.40	36.20	1.16	0.77	0.08	2.34	0.28
V/CH-plasma	2.46	0.69	46.00	1.04	0.85	0.14	2.39	0.57

### 3.4. Thermal Stability

Applied chitosan, ultrasound and plasma treatments cause the lowering of the macromolecule orientation, with the supramolecular structure becoming less ordered, especially for plasma treatments. These changes influence the temperature of degradation for the fibers, as presented in Figure 4. The biocomposite regenerated cellulose/chitosan fibers have a more than 30 °C lower temperature of degradation than the regenerated cellulose fibers, and with the ultrasound or plasma treatments the thermal stability of both fibers decreases. As a result of shorter macromolecules on average (lower DP), a less ordered structure (low  $T_{deg}$  and crystallinity) and the decrease in molecular orientation ( $f_{or}$ ), the thermal stability of the ultrasound or plasma treated fibers is substantially lowered. When chitosan was applied to the regenerated cellulose fibers and treated with ultrasound or plasma, the stability increased when compared to the treated fibers. It is assumed that more interactions between cellulose fragments and chitosan molecules led to new molecular rearrangements and interactions, which slightly improved the determined value of the macromolecular orientation and, consequently, the thermal stability of the fibers.

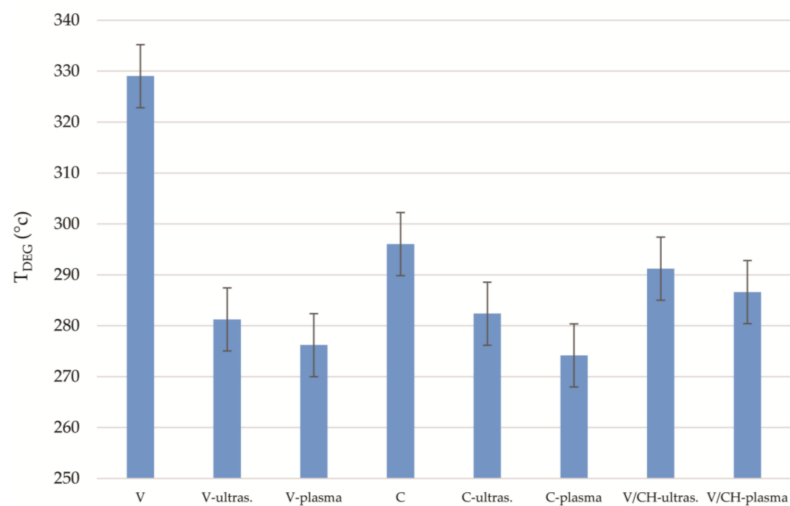


**Figure 4.** Temperature of thermal degradation ( $T_{deg}$ ) for the fibers, with the standard deviation.

### 3.5. Surface Morphology

The morphology for all the fibers was studied with scanning electron microscopy (SEM). Figure 5 shows SEM images of (a) untreated regenerated cellulose fibers, (b) ultrasound treated fibers, and (c) plasma treated fibers. It seemed that with the cavitation effect, ultrasound caused pressure waves in the bath solution, causing surface changes. With etching, plasma also caused surface modifications, such as small damages in the longitudinal direction. The same effect is seen in Figure 6, where biocomposite regenerated/chitosan fibers, treated with plasma and ultrasound, showed similar surface changes and small damages.

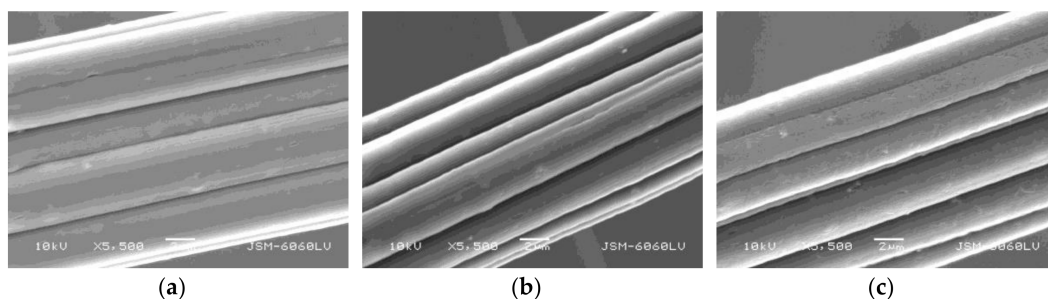


**Figure 5.** Surface of the regenerated cellulose fibers (a) Untreated; (b) Ultrasound treated and (c) Plasma treated; all at a magnification of 5500 $\times$  and a voltage of 10 kV.

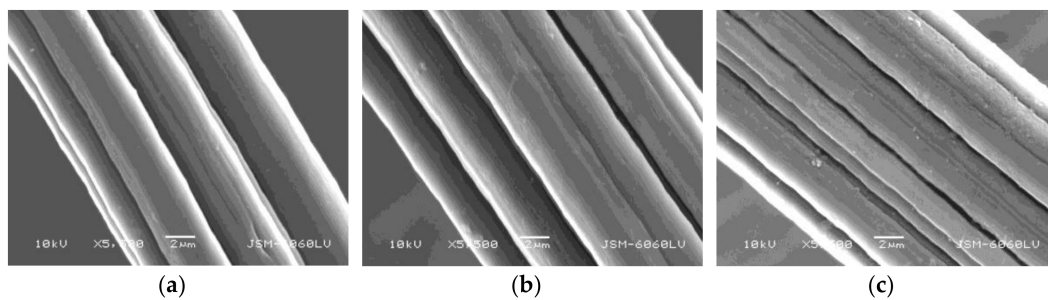


**Figure 6.** The surface of the biocomposite regenerated cellulose/chitosan fibers (a) Untreated; (b) ultrasound treated and (c) plasma treated; all at a magnification of 5500 $\times$  and a voltage of 10 kV.

From Figure 7a, we can conclude that adsorbed chitosan formed small domains on the surface of the cellulose fibers. The behavior and influence of the adsorbed chitosan layer on the surface of the regenerated cellulose fibers was already discussed in this research. Figure 7b reveals fewer agglomerates on the surface of the fibers treated with plasma. The plasma treatment of the regenerated cellulose fibers functionalized by chitosan resulted in a surface that was more even, as was the case for the fibers treated with ultrasound. In these cases, the porous structure of the fiber was less closed, which explains the higher water retention capability and moisture content, when compared with the ultrasound treated fibers.

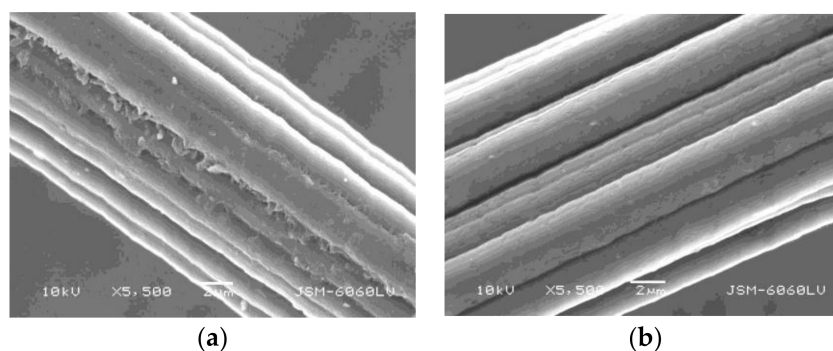


**Figure 7.** Surface of regenerated cellulose fibers firstly treated with chitosan and then with (a) Ultrasound; (b) Plasma; all at magnification 5500 $\times$  and voltage 10 kV.

#### 4. Conclusions

The focus of our research was to apply different treatments onto commercially available regenerated cellulose fibers in order to enhance the sorption properties of fibers, which are used in the hygiene sector. Two different treatments, ultrasound and plasma, were used. Plasma and ultrasound are environmentally friendly processes that could easily be included in the fiber manufacturing process. Two types of fibers were studied, regular regenerated cellulose fibers and biocomposite regenerated cellulose/chitosan fibers.

The study revealed that both treatments, plasma and ultrasound, modify the surface and structure of fibres. The analyses have shown that the treatments cause a lowering of crystallinity, the degree of polymerisation, the molecular orientation and the temperature of degradation, as a consequence of a less ordered structure. The ultrasound treatment had a higher impact on crystallinity, whereas the plasma treatment had a bigger impact on the molecular orientation and structure uniformity, as well as on the surface morphology. These changes resulted in improved sorption properties of the treated fibers.

The functionalization of the regenerated cellulose fibers by chitosan resulted in a more noticeable change in their structure. The ultrasound and plasma treatments enabled the chitosan to chemically attach onto the surface of the fibers. The change in structure and morphology resulted in an improvement of sorption properties and also influenced to some extent their tensile properties. Fibres are more sensitive to tensile loads and are more easily deformed as untreated fibres.

**Acknowledgments:** This work was supported by the Slovenian Research Agency (Programme P2-0213).

**Author Contributions:** Urška Vrabič Brodnjak and Diana Gregor-Svetec conceived and designed the experiments; Urška Vrabič Brodnjak performed the experiments; Urška Vrabič Brodnjak and Diana Gregor-Svetec analyzed the data; Adolf Jesih contributed analysis tools; Urška Vrabič Brodnjak and Diana Gregor-Svetec wrote the paper.

**Conflicts of Interest:** The authors declare no conflict of interest.

## References

1. Božič, M.; Gorgieva, S.; Kokol, V. Laccase-mediated functionalization of chitosan by caffeic and gallic acids for modulating antioxidant and antimicrobial properties. *Carbohydr. Polym.* **2012**, *87*, 2388–2398. [[CrossRef](#)]
2. Pedersen, G.L.; Screws, G.A.; Cedroni, D.M. Biopolishing of cellulosic fabrics. *Can. Text. J.* **1992**, *109*, 31.
3. Anand, S.C.; Kennedy, J.F.; Mirafteb, M.; Rajendran, S. *Medical Textiles and Biomaterials for Healthcare*; Woodhead Publishing Limited: Cambridge, UK, 2005; pp. 90–98.
4. Vrabič Brodnjak, U.; Gregor-Svetec, D. Preparation and characterization of chitosan coatings onto regular cellulose fibers with ultrasound technique. *J. Coat. Technol. Res.* **2013**, *10*, 247–254. [[CrossRef](#)]
5. Bhuiyan, M.R.; Hossain, M.A.; Zakaria, M.; Islam, M.N.; Uddin, M.Z. Chitosan coated cotton fiber: Physical and antimicrobial properties for apparel use. *J. Polym. Environ.* **2017**, *25*, 334–342. [[CrossRef](#)]
6. Ahamed, M.N.; Sankar, S.; Kashif, P.M.; Basha, S.H.; Sastry, T.P. Evaluation of biomaterial containing regenerated cellulose and chitosan incorporated with silver nanoparticles. *Int. J. Biol. Macromol.* **2015**, *72*, 680–686. [[CrossRef](#)] [[PubMed](#)]
7. Ma, B.; Qin, A.; Li, X.; He, C. High tenacity regenerated chitosan fibers prepared by using the binary ionic liquid solvent (Gly·HCl)-[Bmim] Cl. *Carbohydr. Polym.* **2013**, *97*, 300–305. [[CrossRef](#)] [[PubMed](#)]
8. Wang, S.; Lu, A.; Zhang, L. Recent advances in regenerated cellulose materials. *Prog. Polym. Sci.* **2016**, *53*, 169–206. [[CrossRef](#)]
9. Liu, X.D.; Nishi, N.; Tokura, S.; Sakairi, N. Chitosan coated cotton fiber: preparation and physical properties. *Carbohydr. Polym.* **2001**, *44*, 233–238. [[CrossRef](#)]
10. Cao, Z.; Shen, Z.; Luo, X.; Zhang, H.; Liu, Y.; Cai, N.; Xue, Y.; Yu, F. Citrate-modified maghemite enhanced binding of chitosan coating on cellulose porous membranes for potential application as wound dressing. *Carbohydr. Polym.* **2017**, *166*, 320–328. [[CrossRef](#)] [[PubMed](#)]
11. Muxika, A.; Etxabide, A.; Uranga, J.; Guerrero, P.; de la Caba, K. Chitosan as a bioactive polymer: processing, properties and applications. *Int. J. Biol. Macromol.* **2017**, *105*, 1358–1368. [[CrossRef](#)] [[PubMed](#)]
12. Frasc, L.; Ristić, T.; Tkavc, T. Adsorption and Antibacterial Activity of Soluble and Precipitated Chitosan on Cellulose Viscose Fibers. *J. Eng. Fiber. Fabr.* **2012**, *7*, 50–57.
13. Vrabič Brodnjak, U.; Gregor-Svetec, D.; Klančnik, M. Influence of enzymatic treatment on the structural, sorption and dyeing properties of viscose and chitosan/cellulose fibers. *Text. Res. J.* **2016**, *86*, 990–1005. [[CrossRef](#)]
14. Kitkulnumchai, Y.; Ajavakom, A.; Sukwattanasinitt, M. Treatment of oxidized cellulose fabric with chitosan and its surface activity towards anionic reactive dyes. *Cellulose* **2008**, *15*, 599–608. [[CrossRef](#)]
15. Shen, S.S.; Yang, J.J.; Liu, C.X.; Bai, R.B. Immobilization of copper ions on chitosan/cellulose acetate blend hollow fiber membrane for protein adsorption. *RSC Adv.* **2017**, *7*, 10424–10431. [[CrossRef](#)]
16. Shimizu, Y.; Dohmyou, M.; Yoshikawa, M.; Takagishi, T. Dyeing chitin/cellulose composite fibers with reactive dyes. *Text. Res. J.* **2004**, *74*, 34–38. [[CrossRef](#)]
17. HPS, A.K.; Saurabh, C.K.; Adnan, A.S.; Fazita, M.N.; Syakir, M.I.; Davoudpour, Y.; Rafatullah, M.; Abdullah, C.K.; Haafiz, M.K.M.; Dungani, R. A review on chitosan-cellulose blends and nanocellulose reinforced chitosan biocomposites: Properties and their applications. *Carbohydr. Polym.* **2016**, *150*, 216–226.
18. Ahmad, M.; Ahmed, S.; Swami, B.L.; Ikram, S. Adsorption of heavy metal ions: Role of chitosan and cellulose for water treatment. *Langmuir* **2015**, *79*, 109–155.
19. Pillai, C.K.S.; Paul, W.; Sharma, C.P. Chitin and chitosan polymers: Chemistry, solubility and fiber formation. *Prog. Polym. Sci.* **2009**, *34*, 641–678. [[CrossRef](#)]
20. Rinaudo, M. Chitin and chitosan: Properties and applications. *Prog. Polym. Sci.* **2006**, *31*, 603–632. [[CrossRef](#)]
21. Wu, T.; Farnood, R. A preparation method of cellulose fiber networks reinforced by glutaraldehyde-treated chitosan. *Cellulose* **2015**, *22*, 1955–1961. [[CrossRef](#)]
22. Ibrahim, N.A.; Eid, B.M.; Abdel-Aziz, M.S. Effect of plasma superficial treatments on antibacterial functionalization and coloration of cellulosic fabrics. *Appl. Surf. Sci.* **2017**, *392*, 1126–1133. [[CrossRef](#)]
23. Li, X.; Qiu, Y. The application of He/O<sub>2</sub> atmospheric pressure plasma jet and ultrasound in desizing of blended size on cotton fabrics. *Appl. Surf. Sci.* **2012**, *258*, 7787–7793. [[CrossRef](#)]
24. Erra, P.; Molina, R.; Jovic, D.; Julia, M.R.; Cuesta, A.; Tascon, J.M.D. Shrinkage properties of wool treated with low temperature plasma and chitosan biopolymer. *Text. Res. J.* **1999**, *69*, 811–815. [[CrossRef](#)]

25. Perincek, S.; Uzgur, A.E.; Duran, K.; Dogan, A.; Korlu, A.E.; Bahtiyari, İ.M. Design parameter investigation of industrial size ultrasound textile treatment bath. *Ultrason. Sonochem.* **2009**, *16*, 184–189. [[CrossRef](#)] [[PubMed](#)]
26. Shahidi, S.; Ghoranneviss, M.; Sharifi, S.D. Effect of atmospheric pressure plasma treatment/ followed by chitosan grafting on antifelting and dyeability of wool fabric. *J. Fusion Energy* **2014**, *33*, 177–183. [[CrossRef](#)]
27. Jiang, Q.; Yang, G.; Wang, Q.; Sun, Q.; Lucia, L.A.; Chen, J. Ultrasound-assisted xylanase treatment of chemi-mechanical poplar pulp. *BioResources* **2016**, *11*, 4104–4112. [[CrossRef](#)]
28. Alghamdi, A.A.; Abdel-Halim, E.S.; Al-Othman, Z.A. Low-Temperature Bleaching of Cotton Cellulose using an Ultrasound-assisted Tetraacetylenediamine/Hydrogen Peroxide/Triethanolamine System. *BioResources* **2016**, *11*, 2784–2796. [[CrossRef](#)]
29. He, Z.; Wang, Z.; Zhao, Z.; Yi, S.; Mu, J.; Wang, X. Influence of ultrasound pretreatment on wood physiochemical structure. *Ultrason. Sonochem.* **2017**, *34*, 136–141. [[CrossRef](#)] [[PubMed](#)]
30. Tissera, N.D.; Wijesena, R.N.; De Silva, K.N. Ultrasound energy to accelerate dye uptake and dye–fiber interaction of reactive dye on knitted cotton fabric at low temperatures. *Ultrason. Sonochem.* **2016**, *29*, 270–278. [[CrossRef](#)] [[PubMed](#)]
31. Hua, Z.Q.; Sitaru, R.; Denes, F.; Young, R.A. Mechanisms of oxygen-and argon-RF-plasma-induced surface chemistry of cellulose. *Plasmas Polym.* **1997**, *2*, 199–224. [[CrossRef](#)]
32. Prabhu, S.; Vaideki, K.; Anitha, S. Effect of microwave argon plasma on the glycosidic and hydrogen bonding system of cotton cellulose. *Carbohydr. Polym.* **2017**, *156*, 34–44. [[CrossRef](#)] [[PubMed](#)]



© 2018 by the authors. Licensee MDPI, Basel, Switzerland. This article is an open access article distributed under the terms and conditions of the Creative Commons Attribution (CC BY) license (<http://creativecommons.org/licenses/by/4.0/>).